Journal of
Applied and Computational Mechanics

Shahid Chamran
University of Ahvaz

Research Paper

Effect of Throughflow on the Convective Instabilities in an Anisotropic Porous Medium Layer with Inconstant Gravity

D. Yadav[1], A.M. Mohamad[1], G.C. Rana[2]

[1] Department of Mathematical & Physical Sciences, University of Nizwa, Nizwa, P.O. Box 33, PC 616, Sultanate of Oman

[2] Department of Mathematics, NSCBM Govt. College, Hamirpur-177 005, Himachal Pradesh, India

Abstract. The significance of inconstant gravity force and uniform throughflow on the start of convective movement in an anisotropic porous matrix is investigated numerically utilizing large-term Galerkin procedure. The porous layer is acted to uniform upright throughflow and inconstant downward gravitational force which changes with the height from the layer. In this study, two types of gravity field digression were examined: (a) linear and (b) parabolic. It is found that the throughflow parameter Pe, the thermal anisotropy parameter η and gravity deviation parameter λ postpone the beginning of convective activity, whereas the mechanical anisotropy parameter ξ rapids the onset of convective activity. The dimension of the convection cells enhances on enhancing the thermal anisotropy parameter η, the mechanical anisotropy parameter ξ and gravity deviation parameter λ while, the throughflow parameter Pe decreases the extent of the convective cells. It is also noted that the structure with linear variation of gravity force is more stable.

Keywords: Convective instability, Throughflow, Inconstant gravity, Anisotropic porous medium.

1. Introduction

The occurrence of convective motion in a fluid layer depends upon the temperature variance between the fluid layers. If this temperature difference is large enough, then convective motion arises due to buoyancy force. This convective motion builds the arrangement unstable and produces an important phenomenon called convection. The arrival of convective flux in a porous matrix has drawn significant consideration over the last few decades due to its physical uses in several fields such as impurities on water resources, petroleum industry, materials processing, chemical process, Earth's crust and geothermal fields to name a few. For example, the Earth's crust is in a condition of continues flux due to the convective movement in the mantle form new internal crust along midoceanic edges. An motivating problem of convective activity in a porous matrix was evaluated by Horton and Rogers [1]. They found that the critical thermal Rayleigh-Darcy number for the beginning of convective movement is $4\pi^2$. Their outcomes were validated by Elder [2] experimentally. The huge size of research dedicated to this field is well recognized by Ingham and Pop [3], Nield and Bejan [4] and Vafai [5]. Moreover, there have been several investigations concerning convective movement in anisotropic porous matrix [6-15]. Anisotropy is normally an outcome of special direction or uneven geometry of porous medium or fibers and falls in many systems related to engineering and nature.

Throughflow influence on the convective instabilities in an anisotropic porous matrix is important concept since its uses in engineering and geophysics. Higgins [16] and Sherwood and Homsy [17] discussed a new idea in situ coal gasification and suggested that the situ processing of energy resources for instance coal, oil shale, or geothermal energy, contains the convective instabilities with vertical processing (throughflow). The like concerns are also related to processing in packed-bed reactors. Throughflow changes the basic state temperature from linear to nonlinear with layer elevation, which affects the onset of convective instability significantly. The power of throughflow on the beginning of convective instabilities in a porous medium was made by Sutton [18], Homsy [19], Nield [20] and Kiran [21]. They found that the outcome of throughflow does not delay the convective instability always and it depends on the direction of throughflow and character of the boundaries. The case with anisotropic porous medium layer was discussed by Khalili and Huettel [22] and Bhadauria and Singh [23]. They found that a more specific control of the convective instabilities may be reached by alteration of the anisotropy parameters and throughflow strength.

In this paper, we study gravity as a function of height (h) recognized as gravitational force deviation. It is found that the gravitational force of the Earth diverges with height from its planes in a large amount of important circumstances that exists for big scale flows in the geophysical science and engineering, the atmosphere and the sea [24-28]. However, the examination of the consequence of inconstant gravity field on the start of convective movement in a porous layer is very limited. Alex et al. [29] calculated the weight of linear variation of gravity field and interior heat power on the appearance of convective movement in a porous layer and observed that the declining gravity parameter has stabilizing influence on the stability of the arrangement. The

expansion with anisotropic porous matrix was completed by Alex and Patil [30]. The linear and nonlinear digression of gravity strength on the beginning of convective movement in a porous matrix with heat source was explored by Rionero and Straughan [31]. Very recently, Yadav [32] examined the significance of uneven gravity force and even throughflow on the start of convection in a Darcian porous matrix and found that these parameters are to suspend the start of convective activity. The idea of throughflow is applied to manage the convective movement in engineering disciplines, manufacturing and geophysics. The extension with internal heating and rotation were also made by Yadav [33,34].

The literature review demonstrated that till now no attempt has been made about the examination of the start of convective motion in an anisotropic porous medium layer with irregular gravity power and throughflow effects. Such examinations may be helpful to deal the problems associated to large scale flows in the material processing, Earth's crust, atmosphere, ocean, toxin transfer in saturated soils, fuel drilling, in the situ processing of energy resources and crystals augmentation, where throughflow can be vital to manage the convective instability [16, 17, 23-28]. Rao et al. [35] organized a contrast among the parabolic, binomial and exponential variations of gravity field with depth and they achieved that the parabolic function well fits for most crustal structure. In sight of the significance of such a concern, the key intend of the current research is to explore the mutual influence of the throughflow and the changeable gravitational force on the coming of convective movement in an anisotropic porous layer for two sets of functional values of gravity field digression: (a) G(z) = -z (linear) and (b) G(z) = -z² (parabolic). A numerical result of the prevailing equations is offered utilizing large-term Galerkin technique. The significances of numerous applicable parameters on the launch of convective motion are presented in detail.

2. Mathematical Modeling

We considered an infinite extended parallel fluid saturated anisotropic porous layer bounded amid the plates $z = 0$ and $z = h$, and heated from bottom. The physical diagram of the system is exposed in Fig. 1. The layer is acted to a uniform upright throughflow w_c and inconstant gravitational force $\mathbf{g}(z)$ which relays on the vertical part z and works in the opposite z-way. The temperatures at the bottom and upper boundaries are alleged to be θ_1 and $\theta_2 (\theta_2 < \theta_1)$, respectively. Furthermore the Darcy's rule and the Boussinesq–Oberbeck estimation are expected to be effective. The Darcy's law is suitable for slow flow and most groundwater flow cases belong to this category. Whereas the Boussinesq–Oberbeck approximation is applicable for flows that has small variation in temperature. In this way the deviation in density is small and the buoyancy drives the flow. In this manner the variation in density is ignored wherever with the exception in the buoyancy term. With these assumptions, the equations which express the current flows are [36-39]:

$$\nabla . \mathbf{u} = 0 , \tag{1}$$

$$\frac{\mu}{\tilde{\mathbf{K}}} \mathbf{u} = -\nabla P - \rho_0 \left[1 - \beta (\theta - \theta_c) \right] g(z) \hat{\mathbf{e}}_\mathbf{z}, \tag{2}$$

$$\left[(\rho c)_m \frac{\partial}{\partial \tau} + (\rho c)_f (\mathbf{u} \cdot \nabla) \right] \theta = \nabla \cdot \left(\tilde{\mathbf{k}}_m \cdot \nabla \theta \right) . \tag{3}$$

Here, $g(z) = g_0 [1 + \lambda G]$ is the inconstant gravity, G is the functional estimate of gravity field with layer depth z, $\nabla \equiv \hat{\mathbf{e}}_\mathbf{x} \partial / \partial x + \hat{\mathbf{e}}_\mathbf{y} \partial / \partial y + \hat{\mathbf{e}}_\mathbf{z} \partial / \partial z$. All other notations are defined in the nomenclature. The converse of the permeability and the thermal conductivity tensors of the porous matrix are described respectively as:

$$\tilde{\mathbf{K}}^{-1} = K_h^{-1} \left(\hat{\mathbf{e}}_\mathbf{x} \hat{\mathbf{e}}_\mathbf{x} + \hat{\mathbf{e}}_\mathbf{y} \hat{\mathbf{e}}_\mathbf{y} \right) + K_z^{-1} \hat{\mathbf{e}}_\mathbf{z} \hat{\mathbf{e}}_\mathbf{z}, \tag{4}$$

$$\tilde{\mathbf{k}}_m = k_{mh} \left(\hat{\mathbf{e}}_\mathbf{x} \hat{\mathbf{e}}_\mathbf{x} + \hat{\mathbf{e}}_\mathbf{y} \hat{\mathbf{e}}_\mathbf{y} \right) + k_{mz} \hat{\mathbf{e}}_\mathbf{z} \hat{\mathbf{e}}_\mathbf{z}. \tag{5}$$

Here, K_h and K_z are the horizontal and vertical permeability's of the porous matrix, respectively and, k_{mh} and k_{mz} are the horizontal and vertical effective thermal conductivities of porous matrix, respectively. In writing Eqs. (4) and (5), the horizontal mechanical and thermal isotropy are assumed. Eqs. (1)-(3) can be nondimensionalized by taking the subsequent substitution:

$$(x, y, z) = (\hat{x}, \hat{y}, \hat{z}) h, \ \mathbf{u} = \frac{\hat{\mathbf{u}} k_v}{h}, \ \theta = \hat{\theta} \Delta \theta + \theta_c, \ \tau = \frac{h^2 \hat{\tau}}{k_v}, \ P = \frac{\hat{P} \mu k_v}{K_z}, \tag{6}$$
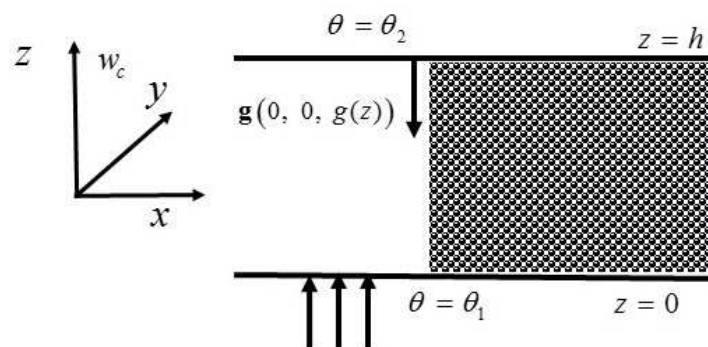

Fig. 1. The physical diagram of the system.

where, $k_v = k_{mz} / (\rho c)_f$, $\Delta\theta = (\theta_1 - \theta_2)$. Then, the nondimensionalize form of Eqs. (1)-(3) after eradicating the pressure term by operating curl two times and using the dimensionless continuity equation $(\widehat{\nabla}.\widehat{\mathbf{u}} = 0)$ are:

$$\widehat{\nabla}_H^2 \hat{w} + \frac{1}{\xi}\frac{\partial^2 \hat{w}}{\partial \hat{z}^2} - R_D \widehat{\nabla}_H^2 \hat{\theta}[1 + \lambda G] = 0, \tag{7}$$

$$\gamma\frac{\partial \hat{\theta}}{\partial \hat{\tau}} + (\widehat{\mathbf{u}} \cdot \widehat{\nabla})\hat{\theta} = \left(\eta\widehat{\nabla}_H^2 + \frac{\partial^2}{\partial \hat{z}^2}\right)\hat{\theta}. \tag{8}$$

Here, $R_D = \rho_0\beta h K_z g_0 \Delta\theta / \mu k_v$, $\eta = k_{mh} / k_{mz}$, $\xi = K_h / K_z$, $\gamma = (\rho c)_m / (\rho c)_f$, $\widehat{\nabla}_H^2 \equiv \partial^2/\partial\hat{x}^2 + \partial^2/\partial\hat{y}^2$, $\widehat{\nabla} \equiv \hat{\mathbf{e}}_x \partial/\partial\hat{x} + \hat{\mathbf{e}}_y \partial/\partial\hat{y} + \hat{\mathbf{e}}_z \partial/\partial\hat{z}$ and $\widehat{\nabla}^2 \equiv \partial^2/\partial\hat{x}^2 + \partial^2/\partial\hat{y}^2 + \partial^2/\partial\hat{z}^2$. The boundary circumstances are:

$$\begin{aligned}\hat{w} = \text{Pe}, \quad \hat{\theta} = 1, \quad \text{at } \hat{z} = 0,\\ \hat{w} = \text{Pe}, \quad \hat{\theta} = 0, \quad \text{at } \hat{z} = 1.\end{aligned} \tag{9}$$

Here $\text{Pe} = hw_c / \alpha_m$. The basic state is taken to be of the form: $\hat{\mathbf{u}}_b = \hat{\mathbf{e}}_z \text{Pe}$, $\hat{\theta}_b = \hat{\theta}_b(\hat{z})$. Then the basic state temperature is given as:

$$\hat{\theta}_b = \frac{e^{\text{Pe}} - e^{\text{Pe}\hat{z}}}{e^{\text{Pe}} - 1}. \tag{10}$$

3. Instability

We now expect very slight perturbations on the basic state as $\hat{\mathbf{u}} = \hat{\mathbf{u}}_b + \mathbf{u}'$ and $\hat{\theta} = \hat{\theta}_b + \theta'$. Here $\mathbf{u}'$ and θ' are perturbed dimensionless velocity and temperature. Substituting these into Eqs. (7) and (8) and linearizing, we obtain the following instability equations:

$$\widehat{\nabla}_H^2 w' + \frac{1}{\xi}\frac{\partial^2 w'}{\partial \hat{z}^2} = R_D \widehat{\nabla}_H^2 \theta'[1 + \lambda G], \tag{11}$$

$$\gamma\frac{\partial \theta'}{\partial \hat{\tau}} + (\mathbf{u}' \cdot \widehat{\nabla})\hat{\theta}_b + (\hat{\mathbf{u}}_b \cdot \widehat{\nabla})\theta' = \left(\eta\widehat{\nabla}_H^2 + \frac{\partial^2}{\partial \hat{z}^2}\right)\theta'. \tag{12}$$

Supposing the perturbation quantities as [40]:

$$(w', \theta') = \left[\hat{w}(\hat{z}), \hat{\theta}(\hat{z})\right]e^{[i(\chi_1\hat{x} + \chi_2\hat{y}) + \sigma\hat{\tau}]}, \tag{13}$$

where, χ_1 and χ_2 are the flat wave numbers and σ is the expansion rate of instability. On substituting Eq. (13) into Eqs. (11) and (12), we have:

$$\left[D^2 - \xi a^2\right]\hat{w} + \xi a^2 R_D \hat{\theta}[1 + \lambda G] = 0, \tag{14}$$

$$-\frac{d\hat{\theta}_b}{d\hat{z}}\hat{w} + \left[D^2 - \eta a^2 - \gamma\sigma - \text{Pe } D\right]\hat{\theta} = 0, \tag{15}$$

where $D \equiv d/d\hat{z}$ and $a = \sqrt{\chi_1^2 + \chi_2^2}$ is the wave number. Now, the boundary settings are:

$$\hat{w} = \hat{\theta} = 0, \quad \text{at } \hat{z} = 0,1 \tag{16}$$

4. Technique of Solution

The system of governing Eqs. (14) and (15) is solved by Galerkin process. So, the variables are defined as:

$$\hat{w} = \sum_{k=1}^{N} A_k \hat{w}_k \text{ and } \hat{\theta} = \sum_{k=1}^{N} B_k \hat{\theta}_k. \tag{17}$$

Here A_k and B_k are unknown coefficients and $\hat{w}_k = \hat{\theta}_k = \sin k\pi\hat{z}$. By means of Eq. (17) into Eqs. (14) and (15) and using the orthogonal property, we have:

$$\begin{aligned}C_{jk}A_k + D_{jk}B_k = 0,\\ E_{jk}A_k + F_{jk}B_k = \sigma G_{jk}B_k.\end{aligned} \tag{18}$$

Here, $C_{jk} = \langle D\hat{w}_j D\hat{w}_k / \xi - a^2\hat{w}_j\hat{w}_k\rangle$, $D_{jk} = \langle a^2 R_D \hat{w}_j\hat{\theta}_k[1 + \lambda G]\rangle$, $E_{jk} = \langle -\hat{\theta}_j\hat{w}_k D\hat{\theta}_b\rangle$, $F_{jk} = \langle D\hat{\theta}_j D\hat{\theta}_k - \eta a^2\hat{\theta}_j\hat{\theta}_k - \text{Pe}\hat{\theta}_j D\hat{\theta}_k\rangle$, $G_{jk} = \langle\gamma\hat{\theta}_j\hat{\theta}_k\rangle$, where $\langle YZ\rangle = \int_0^1 YZ \, d\hat{z}$.

Table 1. Estimate of $R_{D,c}$ and a_c with λ for the nonappearance of throughflow and motion in isotropic porous layer, i.e., Pe $= 0$, $\xi = \eta = 1$ for cases (a) $G(z) = -z$ and (b) $G(z) = -z^2$.

G	λ	Current study		Rionero and Straughan [31]	
		$R_{D,c}$	a_c^2	$R_{D,c}$	a_c^2
(a)	0	39.478	9.872	39.478	9.870
	1	77.080	10.208	77.020	10.209
	1.5	132.020	12.313	132.020	12.314
	1.8	189.908	17.198	189.908	17.198
	1.9	212.281	19.475	212.280	19.470
(b)	0	39.478	9.872	39.478	9.870
	0.2	41.832	9.872	41.832	9.874
	0.4	44.455	9.885	44.455	9.887
	0.6	47.389	9.916	47.389	9.915
	0.8	50.682	9.960	50. 682	9.961
	1	54.390	10.036	54.390	10.034

Table 2. Estimate of $R_{D,c}$ and a_c for various values of Pe and λ at $\xi = 0.7$ and $\eta = 0.6$ for types (a) $G(z) = -z$ and (b) $G(z) = -z^2$.

Pe	λ	For type: (a)		For type: (b)		Pe	For type: (a)		For type: (b)	
		$R_{D,c}$	a_c	$R_{D,c}$	a_c		$R_{D,c}$	a_c	$R_{D,c}$	a_c
0	0	36.604	3.902	36.604	3.902	1.2	38.494	3.969	38.494	3.969
	0.25	41.812	3.904	39.370	3.904		44.553	3.955	41.933	3.955
	0.50	48.672	3.910	42.540	3.908		52.787	3.942	45.983	3.943
	0.75	58.052	3.927	46.194	3.918		64.532	3.932	50.799	3.935
	1.00	71.467	3.969	50.430	3.935		82.346	3.938	56.580	3.932
	1.25	91.575	4.076	55.357	3.963		111.320	4.006	63.574	3.940
0.4	0	36.814	3.910	36.814	3.910	1.6	39.967	4.021	39.967	4.021
	0.25	42.235	3.906	39.759	3.906		46.468	4.002	43.735	4.002
	0.50	49.449	3.906	43.164	3.906		55.395	3.981	48.216	3.983
	0.75	59.452	3.915	47.130	3.910		68.317	3.961	53.603	3.967
	1.00	74.032	3.945	51.778	3.921		88.330	3.953	60.152	3.956
	1.25	96.468	4.040	57.253	3.943		121.861	4.006	68.189	3.956
0.8	0	37.443	3.932	37.443	3.932	2	41.864	4.090	41.864	4.090
	0.25	43.146	3.923	40.610	3.924		48.897	4.064	46.027	4.064
	0.50	50.814	3.917	44.306	3.918		58.660	4.035	51.027	4.038
	0.75	61.596	3.916	48.653	3.915		73.007	4.004	57.107	4.013
	1.00	77.622	3.935	53.809	3.920		95.717	3.981	64.598	3.993
	1.25	102.962	4.017	59.963	3.935		134.970	4.017	73.930	3.984

Table 3. Estimate of $R_{D,c}$ and a_c for various values of ξ and λ at Pe $= 0.8$ and $\eta = 0.6$ for types (a) $G(z) = -z$ and (b) $G(z) = -z^2$.

| ξ	λ	For type: (a)		For type: (b)		ξ	For type: (a)		For type: (b)	
		$R_{D,c}$	a_c	$R_{D,c}$	a_c		$R_{D,c}$	a_c	$R_{D,c}$	a_c
0.25	0	65.464	5.087	65.464	5.087	0.75	36.237	3.865	36.237	3.865
	0.25	75.441	5.076	71.007	5.076		41.756	3.856	39.302	3.857
	0.50	88.856	5.066	77.474	5.068		49.177	3.850	42.879	3.851
	0.75	107.717	5.065	85.082	5.065		59.612	3.849	47.087	3.849
	1.00	135.739	5.091	94.100	5.070		75.122	3.868	52.077	3.853
	1.25	179.989	5.199	104.857	5.091		99.645	3.948	58.032	3.868
0.50	0	44.300	4.277	44.300	4.277	1.0	31.815	3.597	31.815	3.597
	0.25	51.047	4.268	48.047	4.268		36.661	3.589	34.507	3.589
	0.50	60.119	4.260	52.419	4.261		43.178	3.583	37.648	3.583
	0.75	72.875	4.260	57.563	4.259		52.341	3.582	41.343	3.581
	1.00	91.837	4.281	63.663	4.264		65.958	3.600	45.724	3.585
	1.25	121.819	4.369	70.944	4.281		87.476	3.675	50.952	3.600
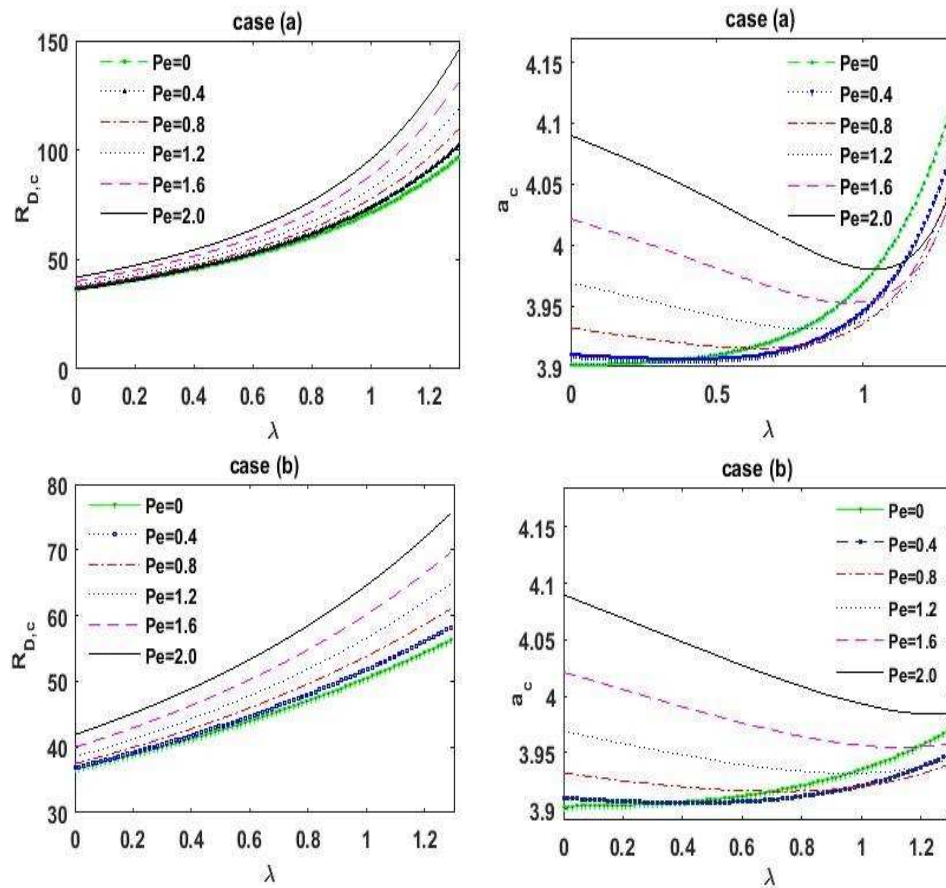
Fig. 2. Estimate of $R_{D,c}$ and a_c with λ for various values of Pe at $\xi = 0.7$ and $\eta = 0.6$ for types (a) $G(z) = -z$ and (b) $G(z) = -z^2$.
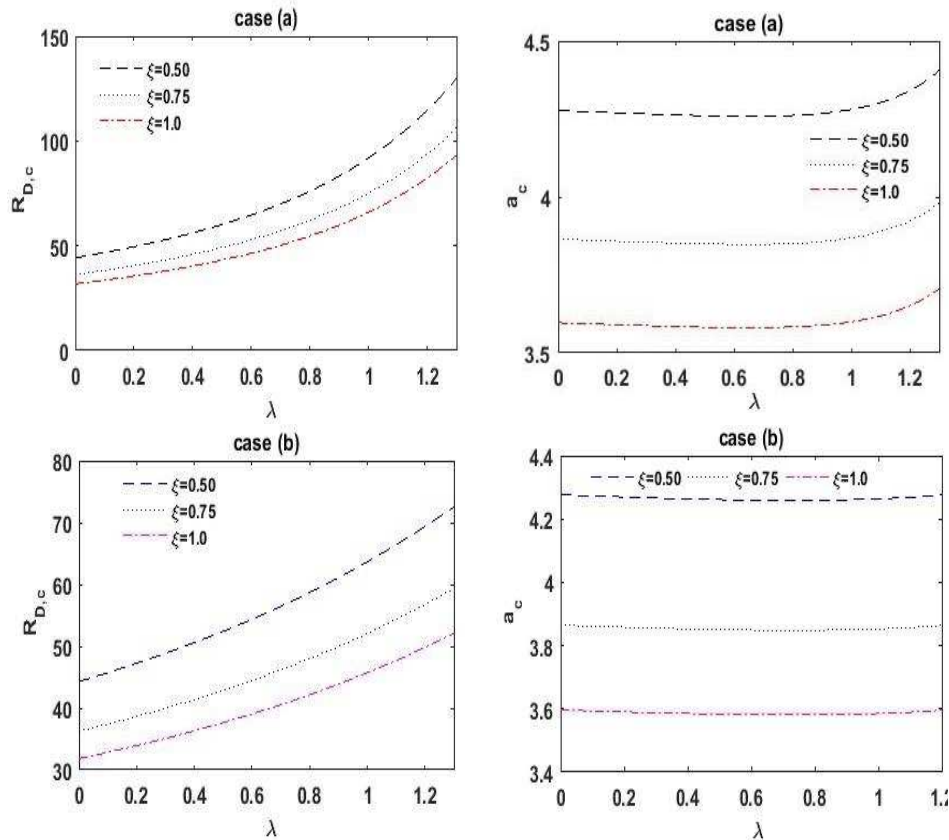

Fig. 3. Estimate of $R_{D,c}$ and a_c with λ for various values ξ at $Pe = 0.8$ and $\eta = 0.6$ for types (a) $G(z) = -z$ and (b) $G(z) = -z^2$.

Table 4. Estimate of $R_{D,c}$ and a_c for various values of η and λ at $Pe = 0.8$ and $\xi = 0.7$ for types (a) $G(z) = -z$ and (b) $G(z) = -z^2$.

η	λ	For type: (a)		For type: (b)		η	For type: (a)		For type: (b)	
		$R_{D,c}$	a_c	$R_{D,c}$	a_c		$R_{D,c}$	a_c	$R_{D,c}$	a_c
0.25	0	25.807	4.895	25.807	4.895	0.75	41.794	3.719	41.794	3.719
	0.25	29.741	4.884	27.994	4.884		48.160	3.711	45.329	3.711
	0.50	35.031	4.875	30.544	4.876		56.719	3.704	49.454	3.705
	0.75	42.468	4.874	33.544	4.873		68.754	3.704	54.307	3.703
	1.00	53.513	4.898	37.099	4.879		86.643	3.722	60.062	3.707
	1.25	70.939	5.005	41.338	4.899		114.930	3.799	66.931	3.722
0.50	0	34.384	4.115	34.384	4.115	1.0	48.601	3.461	48.601	3.461
	0.25	39.621	4.106	37.293	4.107		56.004	3.453	52.713	3.453
	0.50	46.663	4.099	40.687	4.100		65.958	3.447	57.510	3.448
	0.75	56.565	4.099	44.680	4.098		79.954	3.447	63.154	3.446
	1.00	71.282	4.119	49.415	4.103		100.757	3.463	69.847	3.450
	1.25	94.546	4.205	55.065	4.119		133.647	3.535	77.835	3.464

The system of Eqs. (18) forms a generalized eigenvalue situation in σ. The complex eigenvalue σ is achieved in Matlab using QZ procedure and EIG function by fixing the other physical parameters. Then, the nil real portion of σ ($\sigma_r = 0$) is determined by altering R_D using Newton's practice. After that, for recognizing values of a and other fixed parameters, we obtained the imaginary part of σ (σ_i) linked to that valuation of R_D at which σ_r pushes to zero, and approved that the attained estimate of σ_i tends to nil at the same time. We continued this practice for several estimations of a and other prevalent parameters in order to get σ_i all time nil when σ_r tends to nil. Thus, the behavior of the convective motion is stationary for the considered problem.

5. Code Validation

In order to confirm the numerical code, the outcomes obtained by the current technique illustrated in Section 4 are linked to those obtained by Rionero and Straughan [31] in the nonexistence of throughflow and isotropic porous medium (i.e. $Pe = 0$, $\xi = \eta = 1$). The problem is solved for two sets of functional values (a) $G(z) = -z$ and (b) $G(z) = -z^2$ of the variable gravity field using 6-terms Galerkin method. Table 1 shows this comparison for $R_{D,c}$ and a_c^2. The outcomes are provided in the Table 1 exhibit an outstanding agreement with the outcomes obtained by Rionero and Straughan [31]. Hence, it can be stressed that the outcomes which are offered in the subsequent sections are trustworthy.

6. Outcomes and Explanation

This section characterizes the outcomes for the coming of convective motion in the forms of graph (Fig. 2, Fig. 3 and Fig. 4) and Tables (Table 2, Table 3 and Table 4) for Pe, ξ and η as a function of λ. The results show that the stability conditions are given in term of the critical thermal Rayleigh-Darcy number $R_{D,c}$, lower which the arrangement is stable and at the thermal Rayleigh-Darcy number R_D slightly above the critical value of $R_{D,c}$, convective motion occurs in alternating patterns of upward and downward motion.

To evaluate the consequence of Péclet number Pe on the stability of the arrangement, the deviation of $R_{D,c}$ and a_c are displayed in Fig. 2 as a function of λ for types (a) $G(z) = -z$ and (b) $G(z) = -z^2$. The outcomes are also listed in Table 2. From these, it is found that both λ and Pe have a stabilizing outcome on the stability of the arrangement. This may be qualified to the fact that the result of rising λ is to reduce in the gravity strength. Since, the disturbances in the arrangement die down as the gravity strength diminishes and this leads to postponement the start of convective activity. The stability of the system boosts upon increasing Pe. This happened for the reason that the throughflow moves the crucial warmth gradients to the boundary where throughflow is engaged. As a consequence, large values of R_D are needed for the creation of convective activity. The size of the convective cells decreased with the augmentation in the estimates of Pe while it expands with λ. It is also noted that the arrangement shows more stability for case (a).

The result of ξ on the stability of the arrangement is exposed in Fig. 3 and Table 3. From these it is found that the impact of rising ξ hastens the convective wave. This happened because an augment in ξ increases the horizontal permeability which hurries the movement of the fluid horizontally, and consequently smaller estimates of $R_{D,c}$ are needed for the initiate of convective motion with rising ξ. It is also established that a_c reduces as ξ augmented and so its result is to boost the dimension of convection cells. This is for the reason that the slight resistance to horizontal movement also directs to an expansion of the flat wavelength.

The outcome of η on the onset of convective motion is presented in Fig. 4 and Table 4. From these, it is shown that $R_{D,c}$ amplifies on enhancement in the value of η, whereas the critical wave number a_c diminishes on rising η. This exposed that the stability of the arrangement increases with η. This happened for the reason that the flat thermal diffusivity rises with η.

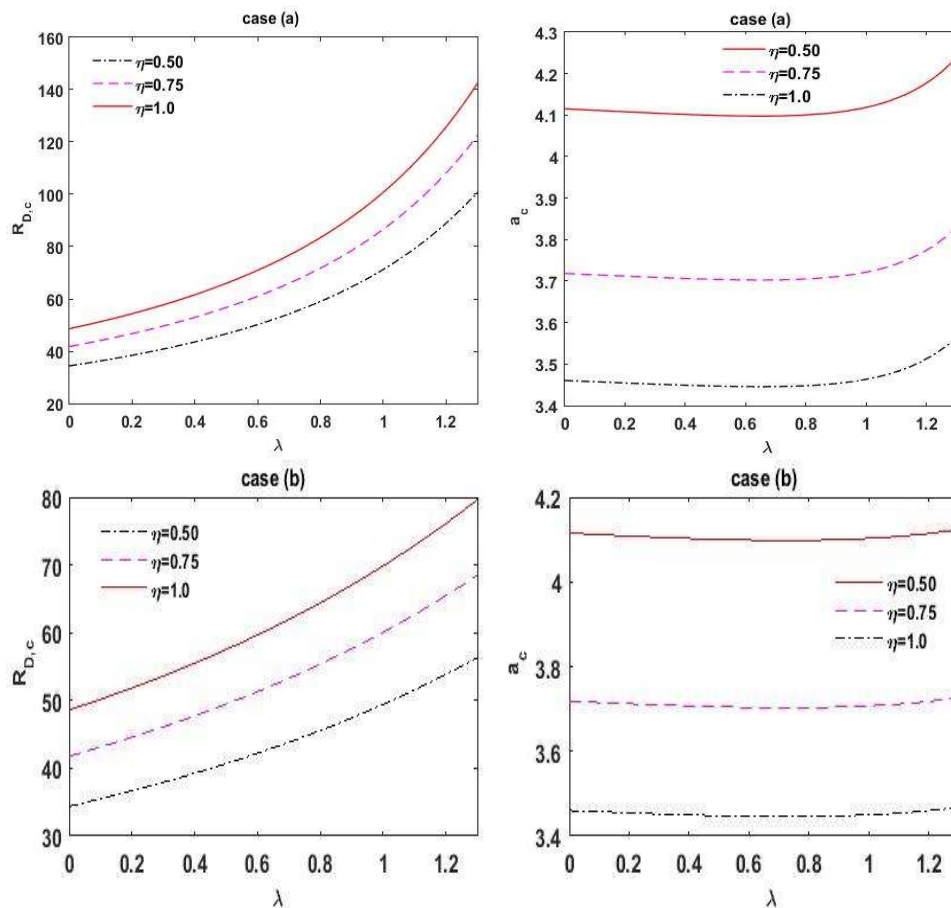**Fig. 4.** Estimate of $R_{D,c}$ and a_c with λ for various values of η at $Pe = 0.8$ and $\xi = 0.7$ for types (a) $G(z) = -z$ and (b) $G(z) = -z^2$.

7. Summary

The significance of the uniform throughflow and the inconstant downward gravity force on the beginning of convective movement in an anisotropic porous layer was inspected numerically utilizing large-term Galerkin process. The inspection was carried out for two varieties of gravity strength digression: (a) $G(z) = -z$ and (b) $G(z) = -z^2$. The main outcomes of the current investigation are as follows:

- The arrangement was found to be more stable on growing η, Pe and λ, while ξ has a destabilizing significant on the stability of the arrangement.
- The measurement of the convective cells decreased on enhancing Pe, for small values of gravity deviation parameter, while it increased with ξ, η and λ.
- The arrangement is more stable for case (a) in comparison to case (b).

Author Contributions

D. Yadav conceived of the presented idea, developed the theory and performed the computations. A.M. Mohamad proof outline and G.C. Rana verified the numerical results. All authors discussed the outcomes and contributed to the final manuscript.

Acknowledgment

Conflict of Interest

The authors declared no potential conflicts of interest related to the research, authorship and publication of this article.

Funding

Nomenclature

a	dimensionless wave number	ρ	density
$\hat{\mathbf{e}}$	unit vector	ε	porosity of the porous medium
$g(z)$	variable gravity	$(\rho c)_f$	heat capacity of fluid

g_0	reference gravity		$(\rho c)_m$	effective heat capacity of porous matrix
h	dimensional fluid layer height		σ	expansion rate of instability
$\tilde{\mathbf{K}}$	permeability tensor of the porous matrix		λ	gravity deviation parameter
$\tilde{\mathbf{k}}_m$	effective thermal conductivity tensor of the porous matrix		ξ	mechanical anisotropy parameter
P	pressure		η	thermal anisotropy parameter
Pe	Péclet number		τ	time
R_D	thermal Rayleigh-Darcy number		θ	temperature
$\mathbf{u}(u,v,w)$	velocity vector		θ_c	reference temperature
w_c	the magnitude of the throughflow velocity		**Superscripts**	
(x,y,z)	space co-ordinates		$'$	perturbed dimensionless quantities
Greek symbols			**Subscripts**	
β	thermal expansion coefficient		0	reference value
∇	del operator		b	basic state
∇^2_H	horizontal Laplacian operator		c	critical
γ	heat capacity ratio		m	effective porous medium
μ	viscosity		f	fluid

References

[1] Horton, C., Rogers, J.F., Convection currents in a porous medium, *Journal of Applied Physics*, 16(6), 1945, 367-370.
[2] Elder, J.W., Steady free convection in a porous medium heated from below, *Journal of Fluid Mechanics*, 27(1), 1967, 29-48.
[3] Ingham, D.B., Pop, I., *Transport Phenomena in Porous Media*, Elsevier, 1998.
[4] Nield, D.A., Bejan, A., *Convection in Porous Media*, Springer, 2006.
[5] Vafai, K., *Handbook of Porous Media*, CRC Press, 2015.
[6] Bég, O.A., Uddin, M.J., BÉG, T., Gorla, R.R., Numerical simulation of self-similar thermal convection from a spinning cone in anisotropic porous medium, *Journal of Hydrodynamics, Ser. B*, 28(2), 2016, 184-194.
[7] Bhadauria, B., Kumar, A., Kumar, J., Sacheti, N.C., Chandran, P., Natural convection in a rotating anisotropic porous layer with internal heat generation, *Transport in Porous Media*, 90(2), 2011, 687.
[8] Capone, F., Gentile, M., Hill, A.A., Penetrative convection via internal heating in anisotropic porous media, *Mechanics Research Communications*, 37(5), 2010, 441-444.
[9] Capone, F., Gentile, M., Sharp stability results in LTNE rotating anisotropic porous layer, *International Journal of Thermal Sciences*, 134, 2018, 661-664.
[10] Castinel, G., Combarnous, M., Natural-convection in an anisotropic porous layer, *International Chemical Engineering*, 17(4), 1977, 605-614.
[11] Degan, G., Vasseur, P., Bilgen, E., Convective heat transfer in a vertical anisotropic porous layer, *International Journal of Heat and Mass Transfer*, 38(11), 1995, 1975-1987.
[12] Kumar, A., Bhadauria, B.S., Thermal instability in a rotating anisotropic porous layer saturated by a viscoelastic fluid, *International Journal of Non-Linear Mechanics*, 46(1), 2011, 47-56.
[13] Mahajan, A., Nandal, R., Anisotropic porous penetrative convection for a local thermal non-equilibrium model with Brinkman effects, *International Journal of Heat and Mass Transfer*, 115, 2017, 235-250.
[14] Malashetty, M.S., Swamy, M., The onset of convection in a binary fluid saturated anisotropic porous layer, *International Journal of Thermal Sciences*, 49(6), 2010, 867-878.
[15] Yadav, D., Kim, M.C., Theoretical and numerical analyses on the onset and growth of convective instabilities in a horizontal anisotropic porous medium, *Journal of Porous Media*, 17(12), 2014, 1061-1074.
[16] Higgins, G., *A new concept for in situ coal gasification: Livermore, Ca*, Univ. Ca., Lawrence Livermore Lab., Rept. UCRL-51217, 1972.
[17] Sherwood, A., Homsy, G.M., *Convective instability during in situ coal gasification*, Lawrence Livermore Lab., 1975.
[18] Sutton, F.M., Onset of convection in a porous channel with net through flow, *Physics of Fluids*, 13(8), 1970, 1931-1934.
[19] Homsy, G.M., Sherwood, A.E., Convective instabilities in porous media with through flow, *AICHE Journal*, 22(1), 1976, 168-174.
[20] Nield, D.A., Convective instability in porous media with throughflow, *AICHE Journal*, 33(7), 1987, 1222-1224.
[21] Kiran, P., Nonlinear throughflow and internal heating effects on vibrating porous medium, *Alexandria Engineering Journal*, 55(2), 2016, 757-767.
[22] Khalili, A., Huettel, M., Effects of throughflow and internal heat generation on convective instabilities in an anisotropic porous layer, *Journal of Porous Media*, 5(3), 2002, 1-12.
[23] Bhadauria, B.S., Singh, A., Throughflow and G-jitter effects on chaotic convection in an anisotropic porous medium, *Ain Shams Engineering Journal*, 9(4), 2018, 1999-2013.
[24] Hirt, C., Claessens, S., Fecher, T., Kuhn, M., Pail, R., Rexer, M., New ultrahigh-resolution picture of Earth's gravity field, *Geophysical Research Letters*, 40(16), 2013, 4279-4283.
[25] Tapley, B.D., Bettadpur, S., Ries, J.C., Thompson, P.F., Watkins, M.M., GRACE measurements of mass variability in the Earth system, *Science*, 305(5683), 2004, 503-505.
[26] Alex, S.M., Patil, P.R., Effect of variable gravity field on soret driven thermosolutal convection in a porous medium, *International Communications in Heat and Mass Transfer*, 28(4), 2001, 509-518.
[27] Olson, P., Silver, P.G., Carlson, R.W., The large-scale structure of convection in the Earth's mantle, *Nature*, 344(6263), 1990, 209-215.
[28] Fedi, M., Cella, F., D'Antonio, M., Florio, G., Paoletti, V., Morra, V., Gravity modeling finds a large magma body in the deep crust below the Gulf of Naples, Italy, *Scientific Reports*, 8(1), 2018, 8229.
[29] Alex, S.M., Patil, P.R., Venkatakrishnan, K., Variable gravity effects on thermal instability in a porous medium with internal heat source and inclined temperature gradient, *Fluid Dynamics Research*, 29(1), 2001, 1.
[30] Alex, S.M., Patil, P.R., Effect of a variable gravity field on convection in an anisotropic porous medium with internal heat source and inclined temperature gradient, *Journal of Heat Transfer*, 124(1), 2002, 144-150.
[31] Rionero, S., Straughan, B., Convection in a porous medium with internal heat source and variable gravity effects, *International Journal of Engineering Science*, 28(6), 1990, 497-503.
[32] Yadav, D., Numerical investigation of the combined impact of variable gravity field and throughflow on the onset of convective motion in a porous medium layer, *International Communications in Heat and Mass Transfer*, 108, 2019, 104274.
[33] Yadav, D., The density-driven nanofluid convection in an anisotropic porous medium layer with rotation and variable gravity field: A Numerical Investigation, *Journal of Applied and Computational Mechanics*, 6(3), 2020, 699-712.
[34] Yadav, D., Numerical solution of the onset of Buoyancy-driven nanofluid convective motion in an anisotropic porous medium layer with variable gravity and internal heating, *Heat Transfer Asian Research*, 2020. https://doi.org/10.1002/htj.21657.
[35] Visweswara Rao, C., Chakravarthi, V., Raju, M.L., Forward modeling: Gravity anomalies of two-dimensional bodies of arbitrary shape with hyperbolic and parabolic density functions, *Computers & Geosciences*, 20(5), 1994, 873-880.

[36] Yadav, D., Bhargava, R., Agrawal, G.S., Boundary and internal heat source effects on the onset of Darcy–Brinkman convection in a porous layer saturated by nanofluid, *International Journal of Thermal Sciences*, 60, 2012, 244-254.

[37] Yadav, D., Kim, M.C., Theoretical and numerical analyses on the onset and growth of convective instabilities in a horizontal anisotropic porous medium, *Journal of Porous Media*, 17(12), 2014, 1061-1074.

[38] Shivakumara, I.S., Dhananjaya, M., Penetrative Brinkman convection in an anisotropic porous layer saturated by a nanofluid, *Ain Shams Engineering Journal*, 6(2), 2015, 703-713.

[39] Yadav, D., The influence of pulsating throughflow on the onset of electro-thermo-convection in a horizontal porous medium saturated by a dielectric nanofluid, *Journal of Applied Fluid Mechanics*, 11(6), 2018, 1679-1689.

[40] Chandrasekhar, S., *Hydrodynamic and Hydromagnetic Stability*, Dover Publication, 2013.

ORCID iD

D. Yadav https://orcid.org/0000-0001-8404-2053

A. M. Mohamad https://orcid.org/0000-0002-3568-1753

G. C. Rana http://orcid.org/0000-0003-2724-8308